RiESTech
Recent in Engineering Science and Technology

MBI

Article

The Effect of Carbon Content on the Biodegradable Metal Foam Fe-35Mn-C Produced by Powder Metallurgy Process with Potassium Carbonate as a Foaming Agent

Yudha Pratesa [1], and Setyaningrum [1,*]

[1] Department of Metallurgy and Material, Faculty of Engineering, Universitas Indonesia, Depok 16424, Indonesia
* Correspondence: yudhapratesa@ui.ac.id

Abstract: A Fe-35Mn-1C alloy with a foam structure, incorporating 5% potassium carbonate (K2CO3), was successfully synthesized, demonstrating an austenite phase and an acceptable degradation rate for an implant candidate. However, excessive carbon content led to the formation of a graphite phase and increasing hardness. To address this, variations in lower carbon composition (0% and 0.5%) were explored to enhance mechanical properties and achieve a fully austenite phase with non-magnetic properties. Mechanical alloying of the powder materials was performed using the rotary mixing method and was followed by sintering process in argon atmopher. The sintered samples underwent comprehensive characterization, including physical, chemical, mechanical properties, and degradation behavior. The Fe-Mn-C biomaterial exhibited an austenite and manganese oxide phase with a favorable degradation rate. This study showed K2CO3 is not only as a foaming agent but also could contribute to carbon alloying into the Fe-Mn alloy system.

Keywords: Potassium Carbonate (K_2CO_3); Carbon; Austenite; Fe-Mn-C

Citation:. Pratesa, Y.; Setyaningrum. (2024). The Effect of Carbon Content on the Biodegradable Metal Foam Fe-35Mn-C Produced by Powder Metallurgy Process with Po-tassium Carbonate as a Foaming Agent, 2(03), 50–59. Retrieved from https://www.-mbi-journals.com/index.php/riest-ech/article/view/72

Academic Editor: Noor Hidayati

Received: 30 July 2024
Accepted: 30 July 2024
Published: 31 July 2024

Publisher's Note: MBI stays neutral with regard to jurisdictional claims in published maps and institutional affiliations.

1. Introduction

Various examples of metallic based biomaterials that are widely used include austenitic stainless steel SS316L, Ni-TiNol, Mg alloys, Co-Cr alloys, Ti alloys, sponge material, and metallic glass. SS316L, as a metallic biomaterial commonly used in biomedical applications, is easy to fabricate, has high corrosion resistance, and is readily available. Austenitic stainless steel has advantages such as good corrosion resistance, high ductility, and diamagnetic properties that do not interfere with MRI examinations [1]. Additionally, Co-based metallic biomaterials, such as Co-Cr-Mo, are widely used in dental applications and artificial joints[2] because they do not contain Ni, which can have adverse effects on the body, have good hardenability, and are non-toxic. Co alloys also have better strength, radiopacity, and corrosion resistance under stress conditions compared to stainless steel[3]. Titanium alloys, which are emerging in the field of biomaterials, have good corrosion resistance and biocompatibility[4], as well as osseointegration properties that allow direct bonding with the human body on a microscopic scale[5].

The development of biodegradable biomaterials for temporary implant applications has significantly advanced over the past few years. These biodegradable materials have proven to address the shortcomings of non-biodegradable biomaterials, such as long-term irritation and chronic inflammation. A biomaterial is considered biodegradable if it can

naturally degrade within the body, is non-toxic, and has optimal corrosion resistance suited to its application. Biodegradable biomaterials for coronary stents must possess excellent mechanical properties and affordable degradation rates. Prolonged presence of stents in the body can lead to adverse effects such as thrombosis and restenosis[6, 7]. Currently, metals like magnesium (Mg)[8] and iron (Fe)[9] are being extensively developed for biodegradable biomaterial applications, often with the addition of other alloys to enhance the desired mechanical properties and characteristics.

Iron (Fe) is a promising alternative for biodegradable biomaterials. In vivo testing has demonstrated that Fe has potential for medical applications requiring degradable materials[10], such as stents implanted in blood vessels. However, pure iron has a drawback of a slow degradation rate for biodegradable biomaterial conditions. To address this, previous research has combined Fe with 35% Mn to increase its degradation rate[11]. Manganese (Mn) also forms an austenite phase, making it safe for magnetic-based medical examinations like MRI.

Previous research has shown that manganese levels correlate with cell viability[11], and were discovered that carbon can substitute for manganese, potentially reducing toxicity levels. Additionally, several various foaming agents has been tested, including carbamide and potassium carbonate[9, 11]. The results indicated that increased carbon content led to the formation of cementite and several ferrite phases. Since a little investigation in powder metallurgy process of FeMnC alloy that used a K_2CO_3 as a foaming agent in the microstructural and phase formation. Therefore, this study aims to investigate the effects of K_2CO_3 addtion as an additional carbon source and foaming agent.

2. Materials and Experiment Methods

The alloy was produced by commercially pure iron (Fe), ferromanganese (FeMn), pure manganese (Mn), pure carbon (C), and potassium carbonate (K_2CO_3) as a foaming agent. Powder metallurgy methods were employed to maintain purity and minimize contamination in the Fe-35Mn-C alloy. This study focused on producing Fe-35Mn-C biomaterials with K_2CO_3 as the foaming agent, varying the carbon content at 0%, 0.5%, and 1%. The materials were mixed using rotary mixing for 2 hours and then compacted using uniaxial isotactic pressing. The compaction of powder mixtures was carried out under a pressure of 200 bars for 15 minutes.

The sintering process was conducted in stages: initial sintering at 850°C for 180 minutes, followed by a secondary sintering at 1100°C for 90 minutes. This approach was used to ensure sample densification before the decomposition of potassium carbonate as the foaming agent. The sintered samples were then characterized, for its microstructure observation with picral etch, density and porosity measurements with an archimedes principle, X ray diffraction hardness, and ion release using Atomic adsoprtion spectosopy after 5 day immerison in Ringer solution with Parkin Elmer Analysis 400.

The physical characterization of the material was determined by measuring density and porosity using the Archimedes principle, in accordance with ASTM A378-88 Standard.

The density testing principle involved comparing the mass of the sample in air to its mass in a fluid. Vegetable oil was used as the fluid to prevent sample corrosion. Density calculations for the material after compaction and sintering were performed using the following equation 1 and 2:

$$\rho_{\text{Archimedes}} = \frac{\text{mass in air}}{\text{mass in fluid}} \quad (1)$$

$$\rho_{teoritical} = (\rho_{Fe}\ x\ \%_{wt\ Fe}) + (\rho_{FeMn}\ x\ \%_{wt\ FeMn}) + (\rho_{C}\ x\ \%_{wt\ C}) + (\rho_{K2CO3}\ x\ \%_{wt\ K2CO3}) \quad (2)$$

The microhardness of the samples after sintering was measured using the Rockwell B method with a load of 100 kgF. Each sample (0% and 0.5% C) was indented five times for a better statistical result. The spacing between indentations was carefully controlled to prevent residual stress that could affect the hardness measurements. Additionally, indentations were made in non-porous areas to ensure the values accurately represented the actual hardness of the samples.

3. Results and Discussion

Physical Characterization : Morphology, Porosity and Density

The observation of porosity in the 0% and 0.5% C samples was conducted visually with an optical macrophoto graph. The porosity morphology of the samples can be seen in the Figure 1. Visual observations revealed that the porosity formed in the 0% C and 0.5% C samples, mixed using a rotary mixer, resulted in smoother and more uniform porosity compared to the 1% C samples mixed manually. This difference is likely due to the more even mixing achieved with the rotary mixer compared to manual mixing with a mortar. The foaming agent K2CO3, which creates pores in the samples, is better distributed and preserved when mixed with a rotary mixer, leading to more consistent and finer pores.

All observed samples exhibited closed-cell foam porosity, where pores are not interconnected. Visual observations showed that samples mixed with the rotary mixer had finer pores than those mixed manually. Optical microscopy, without etching, revealed that porosity became coarser with increasing carbon content, and a more uniform distribution was achieved with rotary mixing compared to manual mixing. This is because K_2CO_3, a hygroscopic compound, remains drier and is better dispersed when mixed using a rotary mixer, as it avoids the mechanical destruction that occurs with manual mixing. K_2CO_3 can easily become wet when exposed to air or in prolonged contact with other materials. The rotary mixing process helps maintain its dryness by minimizing mechanical impact, as the powder is simply placed in a rotating tube

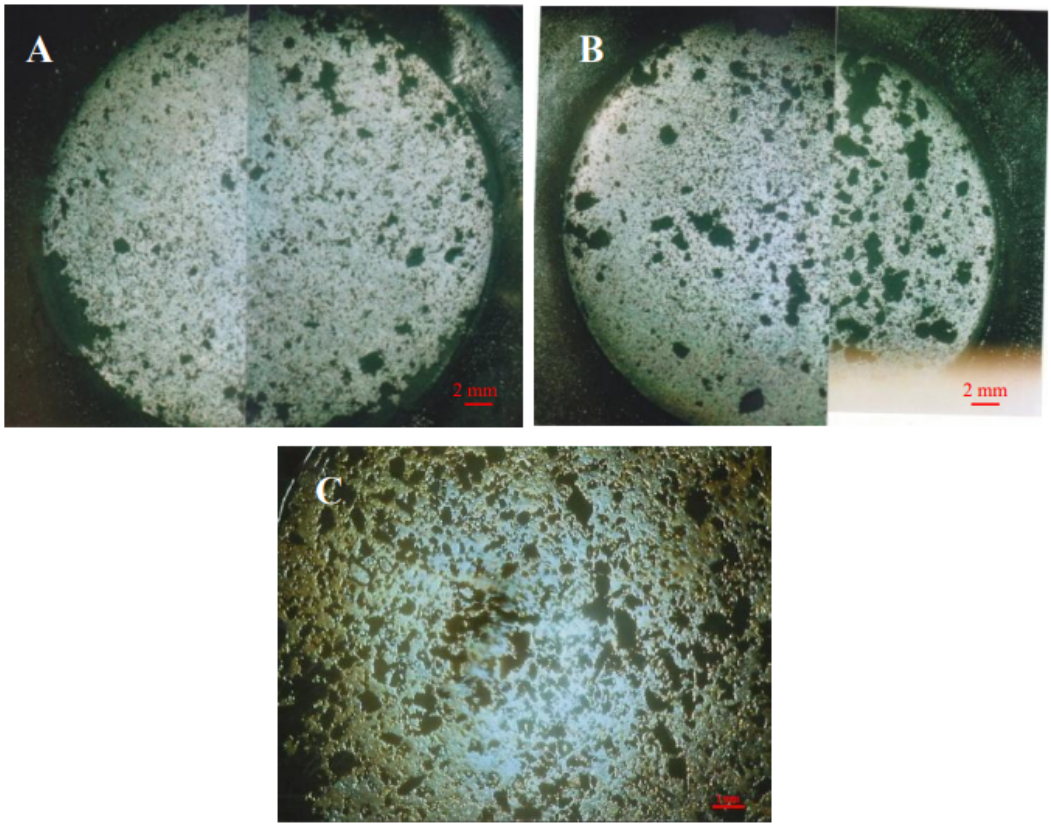

Figure 1. Visual condition of as sintered FeMnC-K_2CO_3 materials with various carbon content (a) 0% c (b) 0.5% and (c) 1% C

Porosity in the 0% C, 0.5% C samples mixed using a rotary mixer, and the 1% C samples mixed manually with a mortar, can arise from three mechanisms. The first mechanism involves the decomposition of the foaming agent K_2CO_3, which starts at 890°C, producing CO_2 gas. This decomposition leaves behind pores and some residual K2O in the sample. In addition to the CO_2 generated by the foaming agent, pores may also form due to inadequate particle bonding during sintering or through the diffusion of Mn into the Fe matrix. Mn diffusion creates pores as it moves towards the sintering atmosphere and then re-diffuses into the Fe matrix.

Density changes in the samples occur due to the formation of foam structure (porosity) after the sintering process. Two types of density were measured to determine the percent porosity of the samples: sample density and theoretical density. Sample density is obtained using Archimedes' principle by comparing the sample's weight in air with its weight in a fluid. Theoretical density is calculated using the Rule of Mixture based on the composition of each sample (0% C, 0.5% C, and 1% C). The density and percent porosity of each sample were calculated. For the sample with 0% C, the sample density was 4.357 g/cm^3 and the theoretical density was 7.361 g/cm^3, resulting in a porosity of 40.8%. For the sample with 0.5% C, the sample density was 4.324 g/cm^3 and the theoretical density was 7.333 g/cm^3, leading to a porosity of 41.0%. In previous research, the sample with 1% C showed similar measurements.

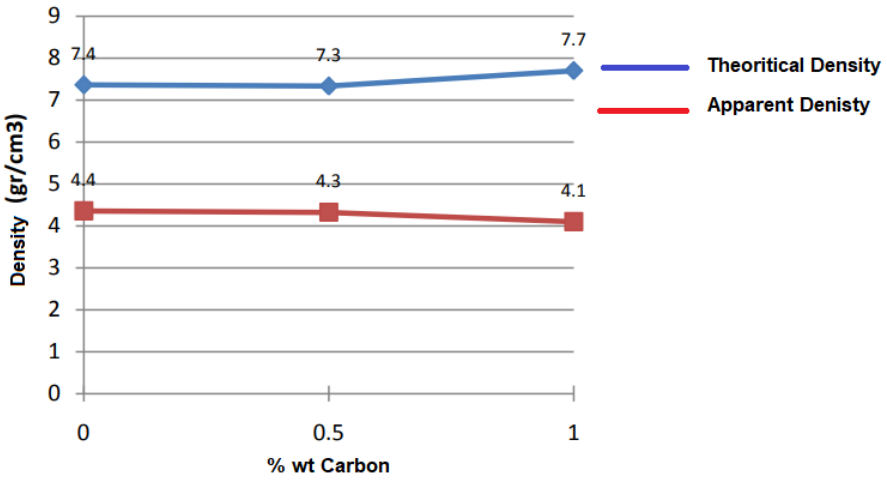

Figure 2. Effect of carbon in density of Fe-Mn-xC

The graph in Figure 2 shows that the theoretical density decreases from the 0% C sample to the 0.5% C sample but increases from the 0.5% C sample to the 1% C sample. This variation is due to differences in the materials used: for the 0% and 0.5% C samples, pure iron (Fe), pure manganese (Mn), pure carbon (C), and K_2CO_3 were used, while for the 1% C sample from previous research, pure iron (Fe), ferromanganese (FeMn), pure carbon (C), and K_2CO_3 were used.

In the current study, the sample densities for 0% and 0.5% C align with the theoretical densities, where density decreases with increasing carbon content. However, the 1% C sample from previous research showed an inverse relationship between sample density and theoretical density. This discrepancy is because the Mn content in the 1% C sample came from FeMn rather than pure Mn. Mn in FeMn has a higher density than pure Mn, resulting in greater porosity and consequently lower sample density

In addition to affecting the sample density after sintering, the addition of carbon (C) and the mixing process also impact the percent porosity. This can be observed in Figure 3. From the porosity percentage graph in Figure 3, it can be observed that the increase in porosity percentage of the Fe35MnC-0.5K2CO3 alloy is more significantly influenced by the mixing process. The samples mixed using a rotary mixer (0% and 0.5% C) exhibit lower porosity percentages compared to those mixed manually (1% C). This is due to the rotary mixing method producing finer pores, meaning that the pore size is smaller, which results in a lower porosity percentage.

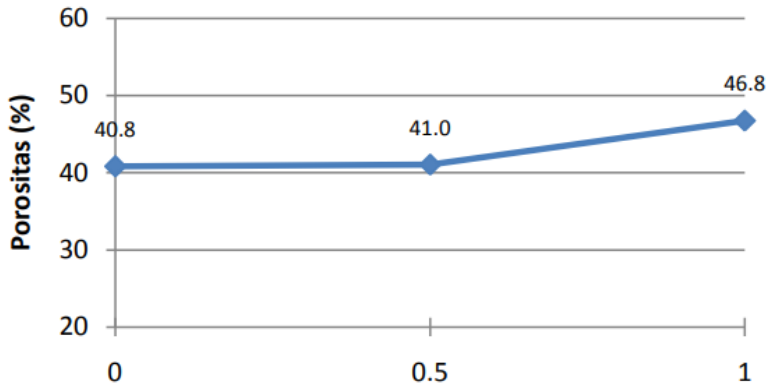

Figure 3. Effect of carbon content ón porosity

Phase analysis

Observations from the 100X magnification microstructure photos indicate that the porosity formed in samples with powder mixing using a lathe machine (0% and 0.5% C) is more evenly distributed compared to samples mixed manually with a mortar as shown in figure 4. As previously mentioned, the mixing process significantly affects the condition of K_2CO_3, the foaming agent. In rotary mixing, K_2CO_3 is more evenly distributed and less damaged due to the absence of impact and air exposure, as the mixing occurs in a closed chamber. The micrographs obtained make it difficult to identify the phases formed in the samples. The challenges in preparing samples with smooth and even surfaces lead to difficulties in optical microscopy due to the high porosity of the samples. Therefore, further testing was conducted.using Xray diffraction.

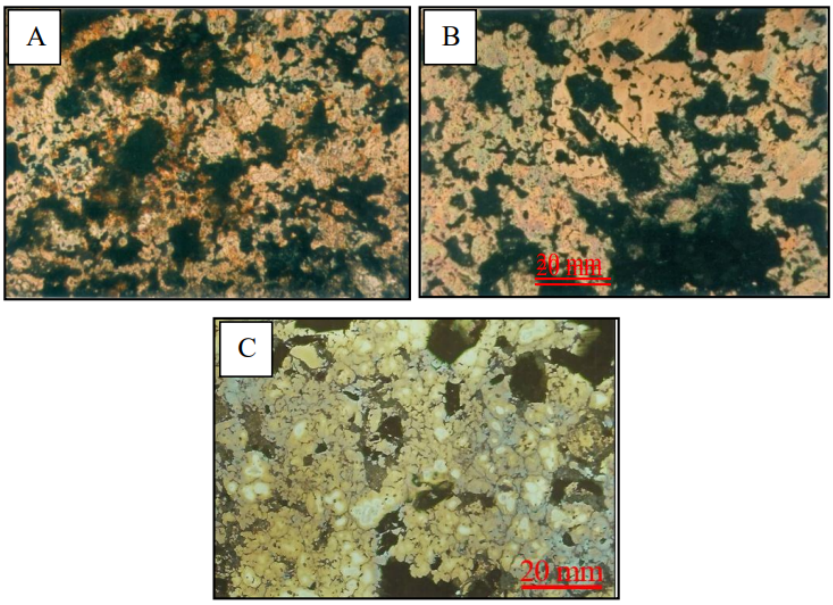

Figure 4. Microstructure of the samples at 100X magnification: (A) 0% C mixed with rotary mixer, etched with Picral+HCl; (B) 0.5% C mixed with rotary mixer, etched with Picral+HCl; (C) 1% C mixed manually, etched with Nital.

The XRD tests revealed that the phases formed in the 0% and 0.5% C samples are austenite (γ) and manganese oxide (MnO), showing consistent trends across samples. These results align with the initial targets and are supported by observations from SEM analysis.

These results indicate that some carbon diffused into the material, originating from the decomposition of K_2CO_3 produced a CO and K2O. The CO will diffuse into the iron powder and make a solid solution with the iron to produce an Austenite phase.

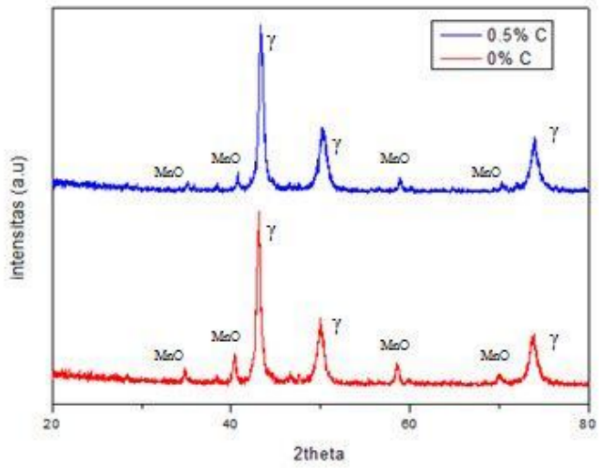

Figure 5. X-ray diffraction result

Hardness Test

The hardness values obtained from the Rockwell B method can be seen in Figure 6. This careful measurement approach ensures that the data accurately reflects the material properties of the sintered samples. It was found that the hardness of the samples increased with the percentage of carbon (C)- In this study, Carbon atoms interstitially integrated into the Fe matrix, causing lattice distortion that impedes dislocation movement, thereby increasing the material's hardness.

Compared to the hardness of SS 316L steel, the hardness values of the samples in this study are much lower. Conversely, the hardness of the 1% C sample is significantly higher than that of SS 316L steel. The hardness values are 28.8 HRB for the 0% C sample, 31.4 HRB for the 0.5% C sample, and 195 HRB for the 1% C sample, while the maximum hardness value for SS 316L steel is 95 HRB. This different phenomena could be related with the cementite formation as mentioned in previous publication.[1]

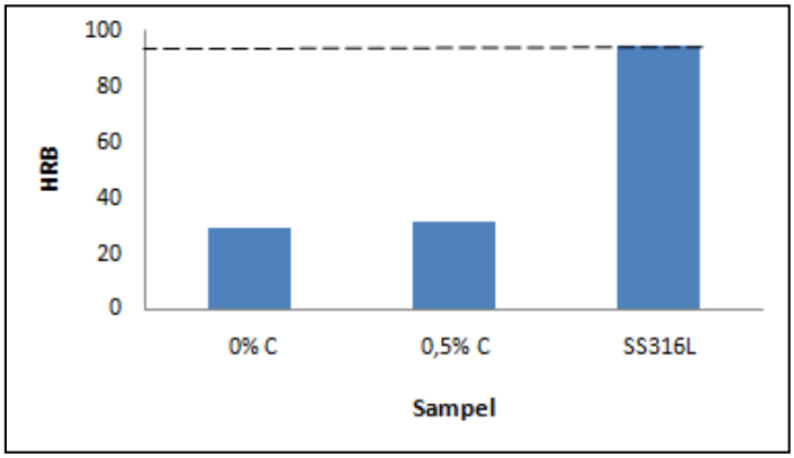

Figure 6. Effect oft he carbon content in FeMnC produced by powder metallurgy

Ion Release

Corrosion testing on the samples was conducted using Atomic Absorption Spectrometry (AAS). This method was chosen over polarization due to the latter's limitations in accurately representing the corrosion rate in porous samples. AAS testing was performed to determine the number of dissolved ions of various elements in samples immersed in Ringer's lactate solution, which simulates body fluid conditions relevant for stent applications. The tests were conducted on the immersion solutions of each sample (0% and 0.5% C) over 1, 3, and 5 days to assess degradation properties. Based on Figure 4.11, it was found that the average dissolved ions of Fe and Mn in all tested sample solutions decreased over time.This result similiar with our previous study.[1]

Based on Figure 7, the average dissolved ions of Fe and Mn in all tested sample solutions decreased from the first day to the fifth day of immersion. This decline indicates a slowing corrosion rate in the samples. The reduced number of dissolved Fe and Mn ions suggests the formation of an oxide layer on the sample surface, which originates from the sample corrosion products and acts as a barrier to further corrosion.

As shown in figure 7, the average dissolved Fe ions decreased daily from 10.4 mg/L after one day of immersion to 5.9 mg/L after three days, and 4.3 mg/L after five days on the 0% C sample,. Similarly, the average dissolved Mn ions in the 0% C sample dropped from 13.5 mg/L after one day of immersion to 5.5 mg/L after three days, and 3.9 mg/L after five days in the Ringer lactate solution. For the 0.5% C sample, the average dissolved Fe and Mn ions also decreased daily. The average dissolved Fe ions in the 0.5% C sample decreased from 11.4 mg/L after one day of immersion to 5.4 mg/L after three days, and 4.3 mg/L after five days. Similarly, the average dissolved Mn ions decreased from 14.3 mg/L after one day of immersion to 5.7 mg/L after three days, and 3.8 mg/L after five days. From the average dissolved Fe and Mn ion data for the 0% and 0.5% C samples, it was found that all measured values remained within safe limits for in-body applications, staying within the daily Uptake Level (UL) .[12,13]

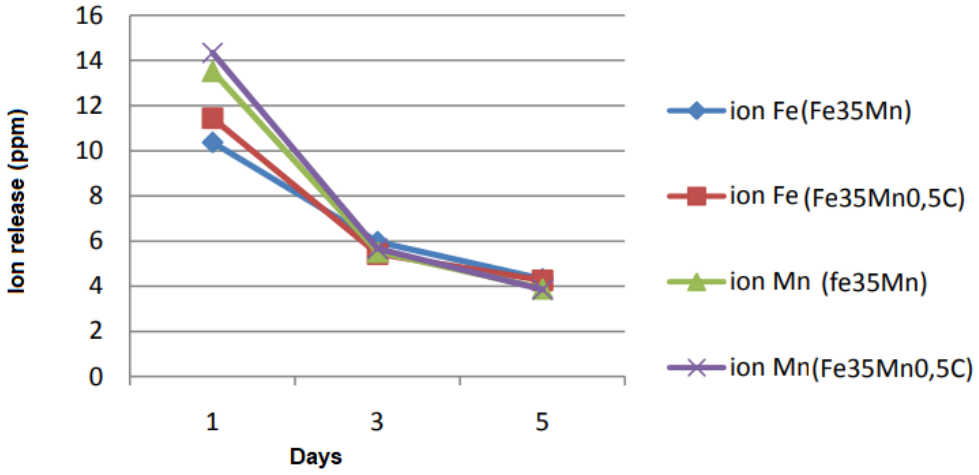

Figure 7. Dissolve ion during the immersion in ringer solution

4. Conclusions

Based on the data and analysis conducted in this study, the following conclusions can be drawn:

- The powder mixing process using the rotary mixing method can refine pore size and reduce the porosity percentage of the Fe35MnC-5%K2CO3 alloy.
- Visual observations revealed that the porosity formed in the Fe35Mn-5% K2CO3 alloy is closed-cell foam.
- Observations using XRD showed the formation of austenite (γ) and manganese oxide (MnO) phases in Fe35MnC-5%K2CO3 with 0%, 0.5%, and 1% C.
- Hardness values obtained through the Rockwell B method indicate that hardness increases with the addition of C, with a hardness of 28.84 HRB for the 0% C sample and 31.42 HRB for the 0.5% C sample.
- The degradation rate of Fe and Mn ions in the Fe35MnC-5%K2CO3 alloy decreases with increased immersion time. The Rockwell B hardness values show an increase in hardness with the addition of C, with the 0% C sample having a hardness of 28.84 HRB and the 0.5% C sample having a hardness of 31.42 HRB.

.

Author Contributions: "Conceptualization, Y.P.; methodology, Y.P.A.; formal analysis, Y.P.; investigation, STN, YP.; writing—original draft preparation, YP.; writing—review and editing, Y.P.; visualization,.

Conflicts of Interest: The authors declare no conflict of interest.

References

1. L.P. Bendel, F.G. Shellock, M. Steckel, The effect of mechanical deformation on magnetic properties and MRI artifacts of type 304 and type 316L stainless steel, Journal of Magnetic Resonance Imaging 7(6) (1997) 1170-1173.
2. M. Grądzka-Dahlke, J.R. Dąbrowski, B. Dąbrowski, Modification of mechanical properties of sintered implant materials on the base of Co–Cr–Mo alloy, Journal of Materials Processing Technology 204(1) (2008) 199-205.
3. R.W.-W. Hsu, C.-C. Yang, C.-A. Huang, Y.-S. Chen, Electrochemical corrosion studies on Co–Cr–Mo implant alloy in biological solutions, Materials Chemistry and Physics 93(2) (2005) 531-538.
4. M. Abdel-Hady Gepreel, M. Niinomi, Biocompatibility of Ti-alloys for long-term implantation, Journal of the Mechanical Behavior of Biomedical Materials 20 (2013) 407-415.
5. D.D. Bosshardt, V. Chappuis, D. Buser, Osseointegration of titanium, titanium alloy and zirconia dental implants: current knowledge and open questions, Periodontology 2000 73(1) (2017) 22-40.
6. R. Iijima, Y. Ikari, E. Amiya, S. Tanimoto, G. Nakazawa, H. Kyono, M. Hatori, A. Miyazawa, T. Nakayama, J. Aoki, The impact of metallic allergy on stent implantation: metal allergy and recurrence of in-stent restenosis, International journal of cardiology 104(3) (2005) 319-325.
7. T. Palmerini, G. Biondi-Zoccai, D.D. Riva, C. Stettler, D. Sangiorgi, F. D'Ascenzo, T. Kimura, C. Briguori, M. Sabatè, H.-S. Kim, A. De Waha, E. Kedhi, P.C. Smits, C. Kaiser, G. Sardella, A. Marullo, A.J. Kirtane, M.B. Leon, G.W. Stone, Stent thrombosis with drug-eluting and bare-metal stents: evidence from a comprehensive network meta-analysis, The Lancet 379(9824) (2012) 1393-1402.
8. I. Karayan, Y. Pratesa, A. Ashari, E. Fadli, D. Nurjaya, Corrosion resistance improvement of ECAP-processed pure magnesium in ringer's solution, Universitas Indonesia (2011) 54-7.
9. Y. Pratesa, B. Suharno, A.C. Wardhana, S. Harjanto, Application of carbamide as foaming agent of Fe-Mn-C alloy for degradable biomaterial candidate with powder metallurgy process, Jurnal Teknologi 81(1) (2019).
10. E. Zhang, H. Chen, F. Shen, Biocorrosion properties and blood and cell compatibility of pure iron as a biodegradable biomaterial, Journal of Materials Science: Materials in Medicine 21 (2010) 2151-2163.
11. J. Syarif, Y. Pratesa, Y. Prasetyo, S. Harjanto, Ball milling effect on corrosion and biocompatibility behavior of FeMnC alloys produced by powder metallurgy in simulated body fluids environment, Metals 11(10) (2021) 1597.
12. S.C.o.t.S.E.o.D.R. Intakes, Dietary reference intakes for calcium, phosphorus, magnesium, vitamin D, and fluoride, (1999).
13. P. Trumbo, A.A. Yates, S. Schlicker, M. Poos, Dietary Reference Intakes - Vitamin A, Vitamin K, Arsenic, Boron, Chromium, Copper, Iodine, Iron, Manganese, Molybdenum, Nickel, Silicon, Vanadium, and Zinc, Journal of the American Dietetic Association 101 (2001) 294-301.